Geochimica et Cosmochimica Acta Vol. 47, pp. 823–839

0016-7037/83/040823-17$03.00/0

Refractory inclusions in the Murchison meteorite

GLENN J. MACPHERSON, MIRYAM BAR-MATTHEWS[1], TSUYOSHI TANAKA[2], EDWARD OLSEN[3] and LAWRENCE GROSSMAN[4]

Department of the Geophysical Sciences, University of Chicago, 5734 South Ellis Avenue, Chicago, Illinois 60637

(*Received June* 23, 1982; *accepted in revised form January* 18, 1983)

Abstract—Mineralogical and petrographic studies of a wide variety of refractory objects from the Murchison C2 chondrite have revealed for the first time melilite-rich and feldspathoid-bearing inclusions in this meteorite, but none of these is identical to any inclusion yet found in Allende. Blue spinel-hibonite spherules have textures indicating that they were once molten, and thus their SiO_2-poor bulk composition requires that they were exposed to higher temperatures (>1550°C) than those deduced so far from any Allende inclusion. Melilite-rich inclusions are similar to Allende compact Type A's, but are more Al-, Ti-rich. One inclusion (MUCH-1) consists of a delicate radial aggregate of hibonite crystals surrounded by alteration products, and probably originated by direct condensation of hibonite from the solar nebular vapor. The sinuous, nodular and layered structures of another group of inclusions, spinel-pyroxene aggregates, suggest that these also originated by direct condensation from the solar nebular gas. Each type of inclusion is characterized by a different suite of alteration products and/or rim layers from all the other types, indicating modification of the inclusions in a wide range of different physico-chemical environments after their primary crystallization. All of these inclusions contain some iron-free rim phases. These could not have formed by reaction of the inclusions with fluids in the Murchison parent body because the latter would presumably have been very rich in oxidized iron. Other rim phases and alteration products could have formed at relatively low temperatures in the parent body, but some inclusions were not in the locations in which they were discovered when this took place. Some of these inclusions are too fragile to have been transported from one region to another in the parent body, indicating that low temperature alteration of these may have occurred in the solar nebula.

INTRODUCTION

CALCIUM-, aluminum-rich inclusions in carbonaceous chondrites have received much attention because of their similarity to predicted refractory condensates from the solar nebula (GROSSMAN, 1972, 1975; LATTIMER and GROSSMAN, 1978) and also because of the unusual isotopic compositions of these objects (LEE, 1979). Most of this effort has been expended on the Type 3 carbonaceous chondrite Allende because of the large size and abundance of inclusions in this meteorite and the large amount of it available for study. Less work has been done on Murchison, a Type 2 carbonaceous chondrite, whose inclusions are smaller and rarer.

FUCHS *et al.* (1973) were the first to describe various inclusion types in Murchison and noted hibonite-bearing, olivine-, pyroxene-bearing and spinel-, pyroxene-bearing inclusions, as well as less refractory objects, all embedded in a phyllosilicate matrix. Later, MACDOUGALL (1979, 1981) and ARMSTRONG *et al.* (1982) described in greater detail other Murchison refractory inclusions which were found by careful inspection of broken surfaces of the meteorite. We have also used this method but, in addition, we have applied a freeze-thaw disaggregation technique which, in combination with heavy liquid separation, allows rapid concentration of large numbers of refractory inclusions. In this way, we have discovered some inclusion types not previously seen in Murchison, such as the corundum-bearing one described previously (BAR-MATTHEWS *et al.*, 1982). This paper gives petrographic and mineralogical descriptions of some other refractory inclusion types that we have found and proposes mechanisms for formation of these objects.

TECHNIQUES

Most inclusions described here were recovered by freeze-thaw disaggregation of the meteorite followed by heavy liquid separation, as described in MACPHERSON *et al.* (1980). All of these were selected on the basis of their bluish color (hibonite) or irregular shape from the densest fraction by hand-picking. In addition, a few inclusions of unusual color or texture were discovered on broken surfaces of the meteorite and these were sampled directly. In many cases, splits of sampled inclusions were taken for trace element analyses whose results will be presented elsewhere.

The remaining portions of the samples were made into polished thin sections and examined optically and with a JEOL JSM-35 scanning electron microscope (SEM). Initial identification of phases was done by examination of their X-ray energy spectra using a KEVEX Si(Li) detector attached to the SEM. Mineral analyses were obtained with an ARL EMX-SM three-spectrometer automated electron microprobe equipped with a Nuclear Semiconductor AUTOTRACE Si(Li) X-ray detector. Both wavelength-dispersive and energy-dispersive analysis methods were used. Well-characterized natural and synthetic minerals and glasses were used as standards. Operating conditions were similar to those described in ALLEN *et al.* (1978).

[1] Present address: Geological Survey of Israel, 30 Malchei Israel Street, Jerusalem, Israel.

[2] Present address: Geological Survey of Japan, Higashi 1-1-3, Yatabe, Ibaraki, 305 Japan.

[3] Also Department of Geology, Field Museum of Natural History, Chicago, Illinois 60605.

[4] Also Enrico Fermi Institute, University of Chicago.

DESCRIPTIONS

Spinel-hibonite spherules

The densest fraction from heavy liquid separation ($\rho > 3.50$) contained tiny blue spherules, ranging from ~70–170 μm in diameter. They consist mostly of spinel and hibonite, lesser perovskite and iron sulfide and rare melilite. These objects are very similar to the refractory spherules described by MACDOUGALL (1981), except for the absence from ours of rims of diopside and iron-rich phyllosilicate. Perhaps the rims are so fragile that our freeze-thaw technique removes them during sample recovery.

Figures 1 and 2 are SEM photographs illustrating some of the textural variety seen in this group of objects. BB-1 (Fig. 1) is concentrically zoned, with a mantle composed mostly of spinel and minor melilite surrounding a core of hibonite and perovskite. Spinel occurs as equant, 5–10 μm-sized colorless crystals that are closely packed against one another. Melilite occurs as sparse, irregularly-shaped grains that are 5–10 μm in size. Accessory melilite has been found in only one other spherule, BB-6. Hibonite occurs as 5 × 20 μm-sized blades, with an intense colorless to blue pleochroism. Where hibonite is intergrown with spinel, the shapes of the spinels are controlled by those of the hibonites. Perovskite occurs as equant, 2–5 μm-sized crystals and is locally enclosed by spinel and hibonite. A peculiar feature of this and other similar inclusions is the presence of numerous small cavities. They constitute 8–10 volume percent of BB-1 and are concentrated mostly in its central region. MACDOUGALL (1981) noted similar cavities in the spheres he examined. In BB-1, the cavities are often associated with melilite and, in such cases, they are irregular in shape. These cavities may have originated by alteration of melilite. Cavities near hibonite are more regular in shape, owing to the euhedral faces of the bounding hibonite blades.

BB-2 (Fig. 2) differs from the previous object in that melilite is absent and euhedral hibonite blades are concentrated in the outer margin, rather than the inner core, of the inclusion. Many hibonites terminate on the inclusion's outer surface and project inward, a feature also noted by MACDOUGALL (1981). Some of the smaller hibonites terminate against the sides of longer ones, suggesting that first-formed crystals obstructed the growth of later ones. This growth interference feature is reminiscent of textures in some Type B inclusions in Allende which were interpreted by MACPHERSON and GROSSMAN (1981a) as objects which were once molten. Perovskite is much less abundant in BB-2 than in BB-1 and is concentrated near the center of the inclusion. As in BB-1, there are numerous small cavities. Some contain tiny crystals of iron sulfide. Larger crystals of the same phase also occur on the inclusion margins. A similar inclusion to BB-2 is BB-4, another in which the hibonites project inward toward the center from the rim. Melilite is again absent.

Yet a third variety of blue spherule is the unique corundum-bearing inclusion, BB-5, noted earlier (BAR-MATTHEWS *et al.*, 1982).

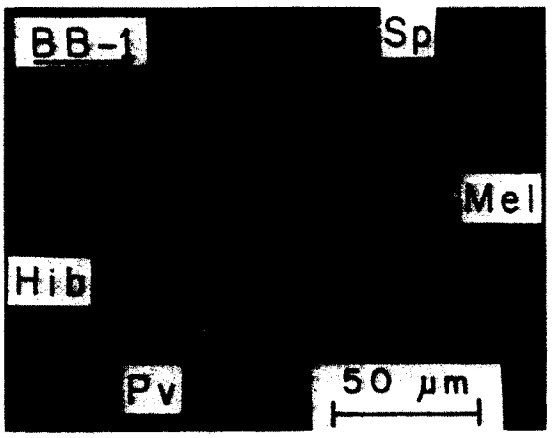

FIG. 1. Back-scattered electron image of a blue spherule, BB-1, showing its concentric zonation. An outer mantle of spinel (Sp), perovskite (Pv) and melilite (Mel) surrounds an inner core of the same phases plus abundant hibonite (Hib). The numerous black areas are cavities.

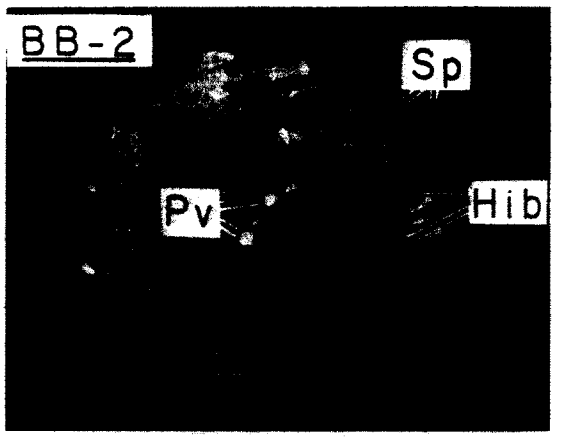

FIG. 2. Back-scattered electron image of the blue spherule, BB-2. Hibonite blades are concentrated towards its outer zone, in contrast to the spherule in Fig. 1. Abbreviations are the same as in Fig. 1. Scale bar is 10 μm.

Melilite-rich inclusions

The $\rho > 3.50$ fraction from heavy liquid separation also yielded three angular fragments, 350–390 μm in maximum dimension, containing melilite as the major phase along with lesser hibonite, spinel and perovskite. The textures of these three fragments are so similar that they are probably pieces of a single broken inclusion.

One of the fragments, labeled MUM (*MU*rchison *M*elilite)-1, is shown in Fig. 3a. The interior of this inclusion, away from the layered rim at the bottom of the photo, consists mostly of blocky melilite crystals up to ~150 μm in length. Optical studies show that these are oriented with their long axes at high angles to the margin of the inclusion, although this is not visible in the SEM view in Fig. 3a. Enclosed by melilite are colorless euhedral spinel crystals (~20 μm), blue to colorless pleochroic, euhedral hibonite blades (~30–40 μm in length) and irregularly-shaped perovskite grains (~1–10 μm). The spinels tend to be slightly rounded and, in places, form long chains. Hibonite and perovskite are sparse in the inclusion interior and are closely associated with spinel. Visible on the right in Fig. 3a are needle-like re-entrants which project inward from the margins of the melilite crystals perpendicular to their length. Small rounded voids within melilite, such as those near the top of Fig. 3a, may simply be cross-sections of the needle-like cavities, visible when the latter are viewed end-on. No secondary minerals have been found in the cavities which, nevertheless, appear to have been produced by corrosion of the melilite. A clearer perspective of the cavities is gained in Fig. 3b, an SEM view of the surface of one of the fragments prior to sectioning. The melilite surface is pitted with planar and rectangular cavities, all of which are empty.

Separating the melilite-rich, coarse-grained interior from the layered rim on each of the MUM fragments is a 30–70 μm-thick region that is rich in spinel, perovskite, hibonite and small (10–15 μm) rounded islands of melilite. The very abundant perovskite grains are enclosed within dense re-

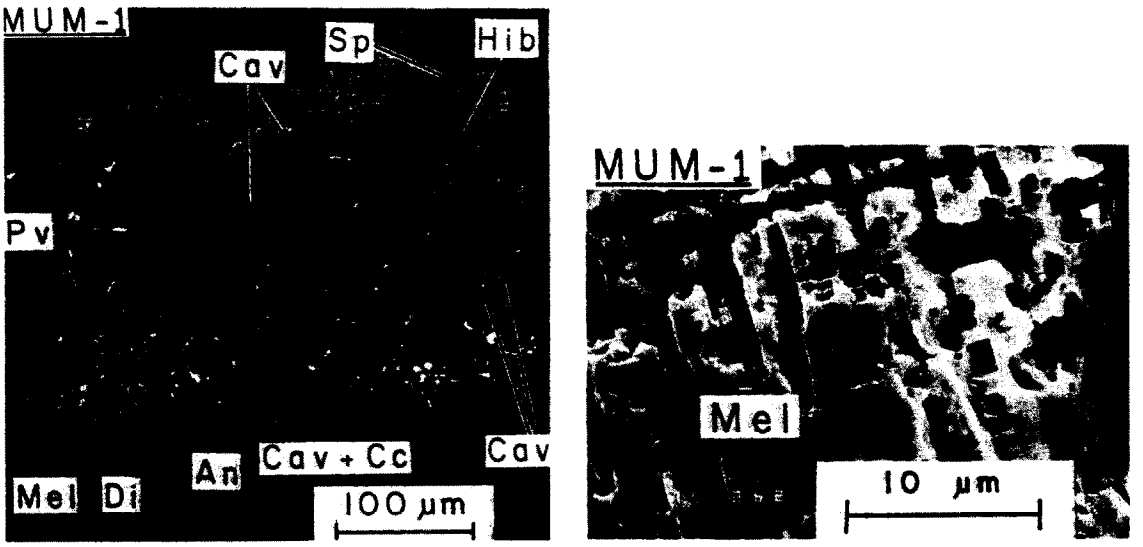

FIG. 3. (a) Back-scattered electron image of a fragment of the melilite-rich inclusion, MUM-1, showing a multi-layered rim sequence surrounding the melilite-rich interior. (b) SEM photograph of the heavily corroded surface of a melilite-rich fragment prior to thin section preparation. Abbreviations are the same as in previous figures except: An—anorthite; Cc—calcite; Cav—cavities; Di—diopside.

gions of spinel and numerous needles and blades (~8–20 μm) of hibonite. It is not known if the small melilite islands are optically continuous with any of the coarse-grained melilites in the inclusion interior. In places, this assemblage is riddled with vermicular cavities. Because many of the melilite islands contain cavities, we suspect that the latter were formed by selective removal of melilite. Associated with the cavities are vermicular patches filled with a mixture of calcium carbonate and an unknown material that is partly iron sulfide. The similarity of their shapes to those of the voids suggests that the patches were once voids that were filled in by a later generation of minerals. The vermicular voids and filled patches are so abundant locally that they give a spongy appearance to these parts of the inclusion.

Mantling the outside of the inclusion is a 25–30 μm-thick, layered rim sequence consisting of the following layers (from inside to outside): Mg-spinel, melilite, anorthite and clinopyroxene that grades outward in composition from Ti-, Al-rich to Ti-, Al-poor. This rim sequence is completely different from the ones on the inclusions described by MACDOUGALL (1979, 1981), as the latter are rimmed either by an Fe, Al, Mg phyllosilicate, diopside and Al, Ti-rich pyroxene; or phyllosilicate and diopside; or phyllosilicate alone; or diopside alone. Because of the freeze-thaw disaggregation process used to obtain this inclusion, we cannot rule out the possibility that there may once have been additional rim layers outside of those now seen in Fig. 3a. We think this possibility unlikely, however, because the outermost rim layer seen on MUM-1 is FeO-poor clinopyroxene, a phase which, when present as a rim layer on the inclusions studied *in situ* by MACDOUGALL (1979, 1981), always constitutes the outermost rim layer.

These melilite-rich fragments are unique among known Murchison inclusions and, in many respects, resemble some Allende compact Type A inclusions (Grossman, 1980). They differ from the latter, however, in their higher hibonite and perovskite contents, different secondary minerals and different rim sequence.

Other hibonite-bearing inclusion types

Two inclusions do not fall into either of the above categories, nor do they precisely resemble any inclusions studied by MACDOUGALL (1979, 1981). They are, however, most similar to MACDOUGALL's (1979) irregularly-shaped spinel- and/or hibonite-bearing (SH) inclusions. Both of our objects were observed on broken fragments of Murchison and, because of their apparently friable nature, were excavated from these specimens directly with stainless steel tools and made into polished thin sections after sampling for trace element analysis.

MUCH-1. Figure 4 is a sketch of the first inclusion, labeled MUCH-1, as it appeared prior to excavation from the meteorite. It is highly irregularly-shaped and consists of a white center and four delicate arms, one of which traces out a semicircular arc and another of which is broken. Each arm contains a central core of blue hibonite, mantled on both sides by white material which, in turn, is coated with a brownish-yellow substance. The entire object is surrounded by black matrix which fills the interstices between the arms. Figure 5 is an SEM view of the thin section made from a portion of this inclusion. From it, we see that the

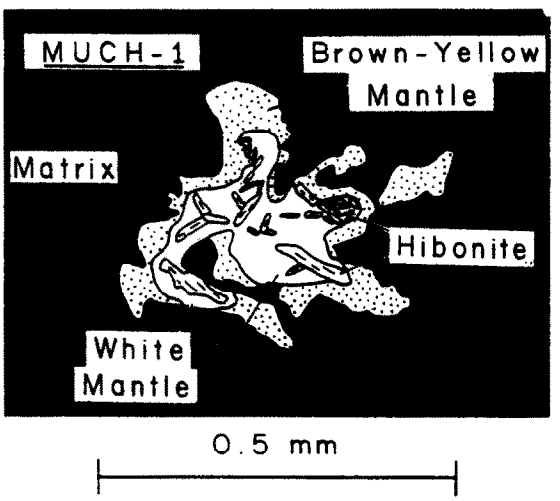

FIG. 4. Line drawing of the inclusion MUCH-1 as it appeared prior to removal from the Murchison meteorite, showing its irregular shape.

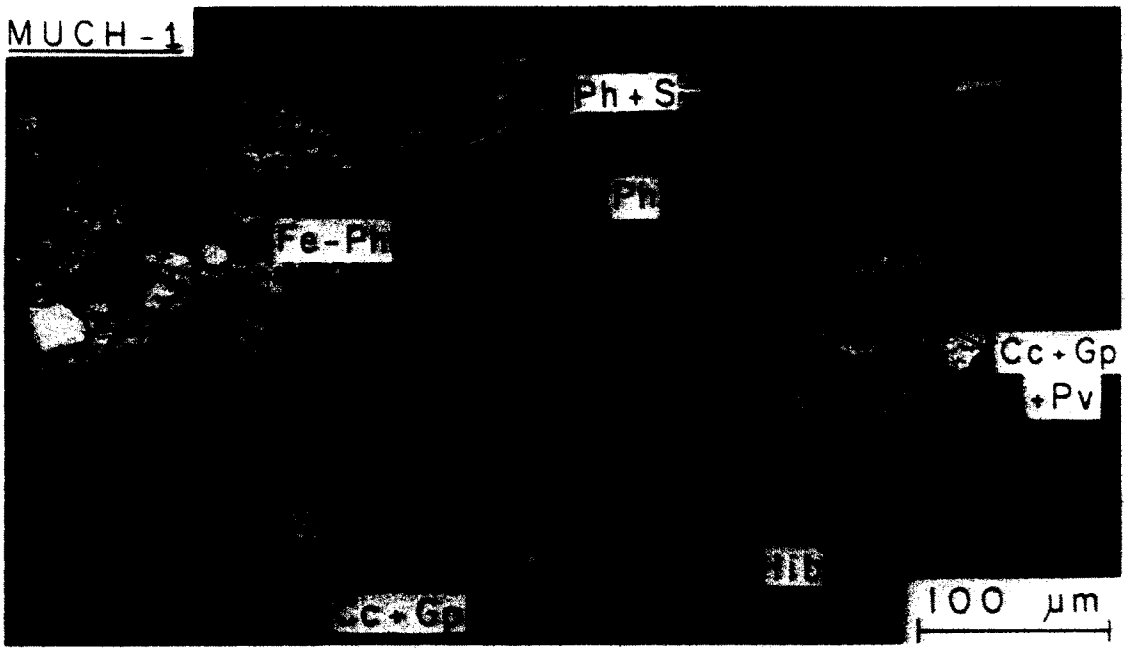

FIG. 5. Back-scattered electron image of MUCH-1 in thin section. The hibonite blades radiate away from a common center, forming a spherulitic cluster. Abbreviations are the same as in previous figures except: Gp—gypsum; Fe-Ph—iron-rich phyllosilicate; Ph—phyllosilicate; S—sulfide.

core of the inclusion is actually an aggregate of hibonite blades, one as long as ~175 μm, that radiate away from a common center in all directions. The outer surfaces of the hibonite blades are somewhat scalloped in appearance at their contact with the white material that rims each of them. This white rim is a 5–10 μm-thick layer of calcite and gypsum, within which are scattered needles (<5 μm) and irregular crystals of perovskite. Perovskite is most abundant at the outer margin of the calcite and gypsum layer, near the contact with the pale brownish-yellow outer rim. This rim actually consists of two parts, the innermost portion being a ~5 μm-thick layer of iron-rich phyllosilicate. Immediately outside of this is a layer of irregular thickness containing Ti-, Al-poor diopside. Figure 5 shows that the phyllosilicate and iron sulfide of the Murchison matrix has a slightly banded structure that wraps around MUCH-1. The portion of the matrix closest to the inclusion is depleted in iron sulfide, and this sulfide-poor region is thickest in the topographic hollows between the hibonite blades. Such a structure is similar to the "clastic rims" described in Allende by MACPHERSON and GROSSMAN (1981b).

Of all the inclusions we have studied, MUCH-1 is the only one which is similar in mineralogy and structure to the Blue Angel inclusion described by ARMSTRONG *et al.* (1982). The latter has a hibonite-rich core, a calcite-rich mantle and an outer, three-layer rim whose major constituents, from inside to outside, are spinel, Fe-rich silicate and Al-diopside. A significant difference between that inclusion and MUCH-1 is that the hibonite in the Blue Angel forms massive, cavity-ridden crystals and clusters of small, euhedral plates, whereas those in MUCH-1 are larger, fewer and form at least one large radial aggregate. Other differences exist in the rims. First, no spinel-rich layer like that in the Blue Angel occurs in MUCH-1 and no phyllosilicate-rich, sulfide-poor outer layer like that on MUCH-1 was found on the Blue Angel. Second, because the rims were deposited on the surfaces of the few, large hibonite crystals making up the radial aggregate that is MUCH-1, the rims mimic this star-like shape rather than form an ovoid shape like that of the mantle of the Blue Angel.

SH-4. The second inclusion, shown in Fig. 6 and labeled SH-4, is one-half of what was once probably a rounded object, ~1.3 mm in diameter. It consists of spinel (2–25 μm), hibonite, fassaite, perovskite, calcite and an unknown feldspathoid-like phase that is much richer in sodium than nepheline. HUTCHEON *et al.* (1980) described this phase as hydrated on the basis of ion microprobe detection of hydrogen in it. The original texture of this inclusion is almost completely obscured by the extreme degree of secondary alteration. A notable feature is the very great abundance of spinel which, wherever it occurs, is euhedral, indicating its resistance to alteration. Hibonite occurs in large clumps of ragged crystals surrounded by abundant perovskite and calcite. The ragged appearance of the hibonite crystals plus the fact that no perovskite occurs *within* the hibonite, suggests that hibonite was altered to form, in part, calcite and pe-

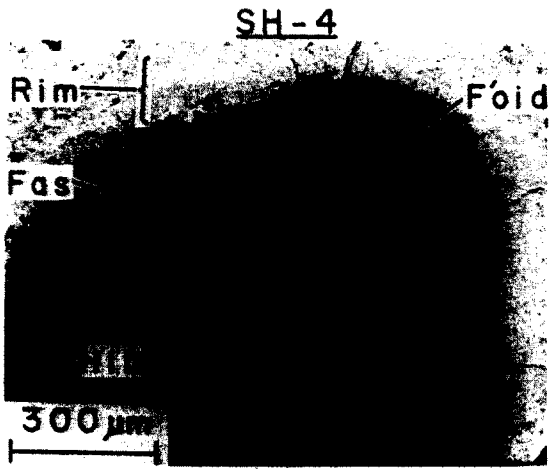

FIG. 6. Back-scattered electron image of inclusion SH-4, showing its rounded shape and numerous dark patches of feldspathoid (F'oid). Fas—fassaite. Other abbreviations are as used previously.

rovskite. Primary fassaite forms rare, blocky to irregularly-shaped crystals (~50–75 μm) with abundant spinel inclusions and very rare perovskite inclusions. Figure 7 shows that surrounding the fassaite are areas composed of spinel, abundant perovskite, the feldspathoid-like phase and calcite. The most plausible interpretation is that the fassaite has been replaced by calcite, perovskite and the feldspathoid but that the spinel has largely resisted alteration.

Large areas within the inclusion consist almost entirely of the feldspathoid-like phase, commonly enclosed within which are numerous euhedral spinels. In other places are cavities lined with successive layers of calcite, diopside and calcite again. Some of these cavities appear to lie within clumps of spinel. At the interfaces between the spinel and the layers lining the cavities are tiny flecks of melilite that are mostly enclosed within the spinel. The melilite-rich zone is concentric with the layers lining the cavities. These cavities associated with melilite are reminiscent of similar structures in BB-1, where cavities are generally associated with or lie within melilite.

Mantling the entire inclusion is a thick (100–150 μm) rim sequence. The inner part consists of two thin (~10 μm), semi-continuous bands, the innermost being spinel and the outer being aluminous diopside. Just to the outside of the diopside, rare crystals (10–20 μm) and crystal clumps of nearly pure forsterite are attached. Surrounding these inner rim bands are two thick (~50 μm each) bands of phyllosilicate, the inner of which is depleted in iron sulfide relative to the outer band. Small crystals of forsterite and pyroxene are scattered within both phyllosilicate bands.

Spinel-pyroxene and olivine-pyroxene inclusions

During freeze-thaw recovery of the refractory inclusions described above, we also found a number of white, botryoidal objects. These contain mostly spinel, olivine and pyroxene, and are free of melilite and hibonite. We have thus far recognized two textural varieties which we call "nodular" and "banded", in reference to their internal structure.

An example of the nodular type, OC-5, is illustrated in Fig. 8. Spinel occurs in rounded clumps, sometimes interconnected, which are mantled by an ~10 μm-thick rim of clinopyroxene that grades outward in composition from fassaite near the spinel to diopside on the outermost edge. A lone grain of forsteritic olivine also occurs in the outermost rim. Enclosed within the spinel are void spaces and rare grains of perovskite and noble metal alloys. Common in some of the voids and also in the outer rim are patches of an iron-rich silicate phase whose composition is similar to the "spinach" phase described by FUCHS *et al.* (1973). Aluminous diopside is also present in most of the voids.

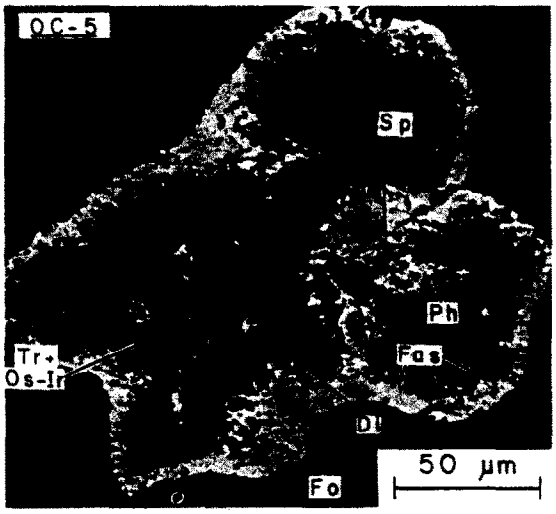

FIG. 8. Back-scattered electron image of inclusion OC-5, showing nodule-like clumps of spinel surrounded by pyroxene rims. Fo—forsterite; Tr + Os-Ir—nugget containing troilite and enriched in osmium and iridium. Other abbreviations are the same as in previous figures.

An example of the banded variety, OC-9, is shown in Fig. 9. Here the spinel is arranged into bands (probably sheet-like structures in the third dimension) with pyroxene mantles. Mineralogically, this inclusion is similar to OC-5, but an olivine outer rim is prominent here. Other similar inclusions also contain rare grains of aluminous enstatite and iron sulfide.

A third variety of botryoidal inclusion, shown in Fig. 10, differs mineralogically from the others in containing abundant olivine and clinopyroxene, but no spinel. Texturally, this particular inclusion, OC-1, is intermediate between the banded and nodular types, as the olivine and pyroxene segregations form band-like structures in some places and nod-

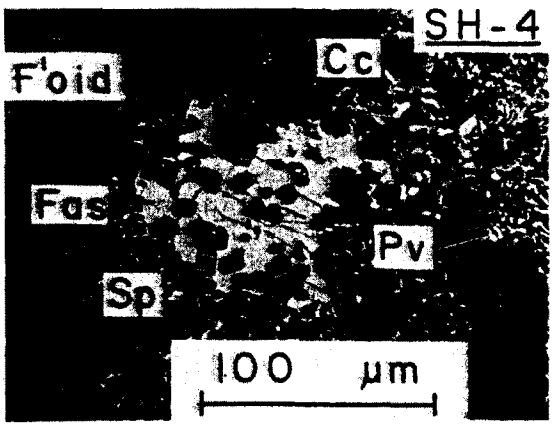

FIG. 7. Back-scattered electron image of a portion of SH-4, showing a fassaite crystal surrounded by an intergrowth of spinel, perovskite, calcite and feldspathoid. Abbreviations are the same as in previous figures.

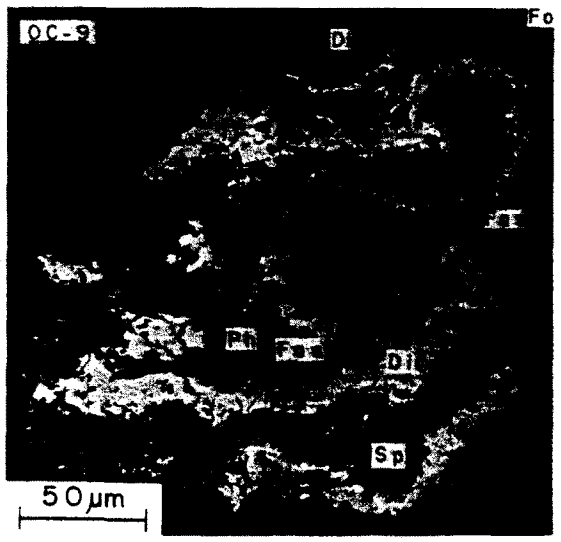

FIG. 9. Back-scattered electron image of inclusion OC-9, showing its spinel, pyroxene and olivine bands. Abbreviations are the same as in previous figures.

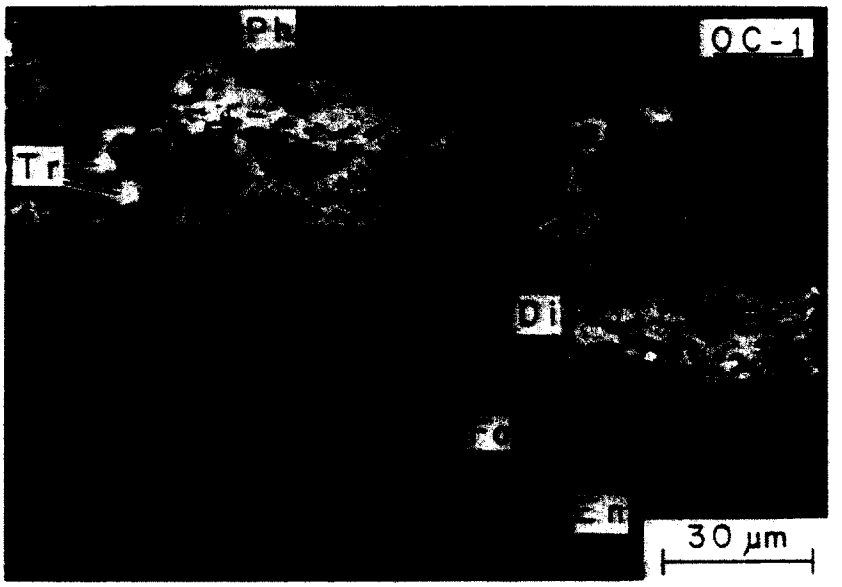

FIG. 10. Back-scattered electron image of the olivine-pyroxene inclusion, OC-1. En—enstatite. Other abbreviations as used previously.

ules in others. As in all other inclusions described in this section, void spaces are prominent. Some of the voids, particularly those associated with cracks, may be due to plucking during polishing of the thin section. A large rounded void near the upper left portion of the photo, however, is significant because a pyroxene band wraps partially around it. Although this void might be interpreted as an artifact of the thin section-making process, its occurrence near a kink in the band seems highly coincidental. Either the void is a primary feature or else it occupies a space formerly filled by an unknown material that has been completely removed by the thin-sectioning process. Similar structures have been found in other banded inclusions, without any trace of an original mineral. We therefore believe that at least some of the void spaces in these inclusions are primary.

Individual hibonite and spinel crystals

The densest fraction from our heavy liquid separates also contained individual crystals of blue hibonite and red and pale blue spinel which were easily recognized because of their colors. We sampled six hibonite and seven spinel crystals by hand and prepared polished grain mounts for petrographic, electron microprobe and ion microprobe study.

Under a dissecting microscope, the hibonites, labeled DJ-1 through DJ-6, are seen to be jewel-like blades, sky blue in color and between 80 and 130 μm in maximum dimension. The crystals are free of obvious inclusions and attached surface material. SEM studies showed that some crystals do contain micron-sized inclusions of perovskite which, in some cases, are euhedral and crystallographically aligned within the host hibonite. Other hibonite crystals are completely free of inclusions. One, DJ-3, has a thin (2–10 μm) partial rim of chromium-rich (2% Cr_2O_3) spinel. The surface of the hibonite at its contact with the spinel is irregular and bumpy, suggesting that the spinel is actually replacing the hibonite.

The spinel crystals, labeled SP-1 through SP-7, are of three types. Only one individual of the first type was studied. It, SP-1, is a perfect octahedron, free of adhering material, pale blue in color and 160 μm in maximum dimension. A dark red variety occurs as 130–200 μm-sized crystals that are enriched in both chromium and iron (*see* Mineral Chemistry). The third variety occurs as pale pink crystals, 150–250 μm in size, and has lower chromium and iron contents than the red spinel. The grains of red and pink spinel range in shape from angular fragments to euhedral crystals. Aluminous diopside occurs as inclusions within some pink spinel crystals and as a rim on another, SP-6. One red spinel contains forsterite inclusions with rims of aluminous diopside separating them from the spinel. Zoning in the spinel is slight, where present, and may be either patchy or concentric. In the concentrically-zoned crystals, the rims are enriched in iron and chromium relative to the cores.

MINERAL CHEMISTRY

Hibonite

Analyses of hibonite from a number of different inclusion types are given in Table 1. The chief variation is in the extent of the coupled substitution

$$Ti^{4+} + Mg^{2+} \rightleftharpoons 2Al^{3+}.$$

The major element contents of hibonite in blue spherules span almost the complete spectrum reported for meteoritic hibonite (*e.g.*, KEIL and FUCHS, 1971; ALLEN *et al.*, 1978; MACDOUGALL, 1979) except for that in the Murchison Blue Angel inclusion (ARMSTRONG *et al.*, 1982) which differs from the rest in having a high V content. In fact, this range can be found in the hibonites from a single inclusion, BB-4 (Table 1, #4, 5). In contrast, all hibonite crystal fragments (DJ's) are uniformly low in TiO_2 and MgO as are the five hibonite analyses from MUCH-1, one of which was selected for Table 1 (#6). The V contents of hibonite grains so far analyzed by us in Murchison are all lower than those reported from Allende either by us (ALLEN *et al.*, 1978; unpublished data) or others (EL GORESY *et al.*, 1980). The only other V data published for Murchison hibonite are those from the

TABLE 1
Electron microprobe analyses of hibonite from refractory inclusions in Murchison

	1	2	3	4	5	6	7	8	9
SiO_2	0.34	0.30	0.42	0.25	0.55	n.d.*	0.33	<0.02	<0.02
Al_2O_3	80.95	78.78	80.04	89.48	79.90	86.46	76.62	89.56	88.68
TiO_2	5.88	7.73	7.36	0.63	6.66	2.05	8.12	2.14	1.92
MgO	3.12	4.47	4.45	1.13	4.62	1.07	4.41	0.77	0.69
CaO	7.84	8.52	8.21	8.32	8.20	8.70	8.58	7.90	7.84
V_2O_3	0.16	n.d.	n.d.	n.d.	n.d.	n.d.	n.d.	<0.02	<0.02
FeO	<0.03	n.d.	n.d.	n.d.	n.d.	n.d.	n.d.	<0.03	<0.03
Sc_2O_3	0.01	n.d.	n.d.	n.d.	n.d.	n.d.	n.d.	0.11	0.07
Total	98.30	99.80	100.48	99.81	99.93	98.28	98.06	100.51	99.20
	Cations per 19 oxygens								
Mg	0.533	0.757	0.746	0.188	0.778	0.181	0.761	0.128	0.115
Ca	0.962	1.036	0.990	0.995	0.994	1.062	1.064	0.940	0.944
Fe	---	---	---	---	---	---	---	0.001	---
Si	0.039	0.034	0.047	0.028	0.062	---	0.038	0.001	---
Al	10.933	10.544	10.615	11.771	10.648	11.605	10.457	11.710	11.744
Ti	0.507	0.660	0.623	0.052	0.567	0.176	0.707	0.179	0.162
V	0.015	---	---	---	---	---	---	0.001	---
Sc	0.001	---	---	---	---	---	---	0.011	0.007
Total Cations	12.990	13.031	13.021	13.034	13.049	13.024	13.027	12.961	12.972

Analyses 2-7 by energy dispersion; 1, 8-9 by wavelength dispersion.
(1,2) BB-1; (3) BB-2; (4,5) BB-4; (6) MUCH-1; (7) SH-4; (8) DJ-3; (9) DJ-6.
*n.d. - not detected. Detection limits for minor elements analyzed by wavelength dispersion are (3σ): Sc - 140 ppm, Fe - 240 ppm, V - 150 ppm, Si - 200 ppm.

Blue Angel (ARMSTRONG *et al.*, 1982) which are mostly much higher than all of those analyzed in this study.

Spinel

Analyses of spinel from five inclusions and of the individual blue octahedron are given in Table 2. No significant differences in composition are evident between any of these spinels. They are nearly pure $MgAl_2O_4$, with only trace amounts of TiO_2, V_2O_3 and FeO. Minor element contents fall near the low ends of the ranges of those in spinel from most Allende coarse-grained inclusions (GROSSMAN, 1975; MACPHERSON and GROSSMAN, 1981a). Vanadium is markedly lower than in spinel from Allende fluffy Type A inclusions, which commonly has $V_2O_3 > 0.5$ wt% (ALLEN *et al.*, 1978; GROSSMAN, 1980).

TABLE 2
Electron microprobe analyses of spinel from refractory inclusions in Murchison

	1	2	3	4	5	6
SiO_2	0.07	n.d.*	0.02	n.d.	0.67	n.d.
Al_2O_3	71.50	72.38	71.44	71.10	68.65	71.88
TiO_2	0.31	n.d.	0.30	0.23	0.27	n.d.
MgO	26.85	27.95	27.52	28.40	27.11	28.41
CaO	0.16	n.d.	n.d.	n.d.	0.59	n.d.
V_2O_3	0.22	n.d.	0.24	n.d.	0.23	n.d.
FeO	0.03	n.d.	0.13	n.d.	0.04	n.d.
Total	99.14	100.33	99.65	99.73	97.56	100.29
	Cations per 4 oxygens					
Mg	0.956	0.982	0.976	1.006	0.983	1.000
Al	2.013	2.012	2.003	1.991	1.969	2.000
V	0.004	---	0.005	---	0.005	---
Ti	0.006	---	0.005	0.004	0.005	---
Fe	0.001	---	0.003	---	0.000	---
Si	0.002	---	---	---	0.016	---
Ca	0.004	---	---	---	0.015	---
Total Cations	2.986	2.994	2.992	3.001	2.993	3.000

Analyses 1 and 5 by wavelength dispersion; others by energy dispersion.
(1) BB-1; (2) BB-2; (3) SP-1; (4) MUM-3; (5) OC-5; (6) OC-9.
*n.d. - not detected. Detection limits for minor elements analyzed by wavelength dispersion are (3σ): Fe - 250 ppm, V - 120 ppm, Ti - 230 ppm.

The individual grains of red and pink spinel gave unsatisfactory microprobe analysis totals due to their rounded surfaces. Nonetheless, the red grains contain 6–7% FeO and 15–24% Cr_2O_3, while the pink grains have ≲0.5% FeO and 1.5–4% Cr_2O_3.

Melilite

Analyses of melilite from a spinel-hibonite spherule, BB-1, and the interiors of two fragments of the melilite-rich inclusion are given in Table 3. All of the melilite is iron- and sodium-free, and has a high Al/Mg ratio (Åk 0–25), similar to melilite in Allende fluffy Type A inclusions but more aluminum-rich than that in Allende compact Type A's (MACPHERSON and GROSSMAN, 1979). The melilite grains in both BB-1 and BB-6 are so small that few high quality analyses could be obtained from them, so no statement can be made regarding melilite composition variations in the spherules. In the melilite-rich inclusions, melilite in the interiors ranges from Åk 2 to Åk 23 and that on the inclusion rims ranges from Åk 3 to Åk 25.

Olivine

Analyses of olivine from a spinel-pyroxene (#2) and an olivine-pyroxene (#1) aggregate are given in

TABLE 3

Electron microprobe analyses of melilite from refractory inclusions in Murchison

	1	2	3	4	5
SiO_2	21.44	25.40	22.68	22.06	27.66
Al_2O_3	36.47	30.62	35.71	37.02	27.68
MgO	0.96	3.02	0.80	0.24	3.60
CaO	39.77	40.74	40.79	40.73	40.90
Na_2O	n.d.*	0.23	0.25	n.d.	n.d.
Total	98.64	100.01	100.23	100.05	99.85
	Cations per 7 oxygens				
Si	0.991	1.160	1.033	1.006	1.262
Al	1.987	1.648	1.918	1.989	1.488
Mg	0.066	0.206	0.055	0.016	0.245
Ca	1.970	1.993	1.991	1.989	1.999
Na	---	0.021	0.022	---	---
Total Cations	5.014	5.028	5.019	5.000	4.994
Åk† (mole %)	0.3	16.8	3.7	0.6	25.9

All analyses by energy dispersion.
(1) BB-1; (2,3) MUM-2; (4,5) MUM-1.
*n.d. - not detected.
†Average åkermanite content from Si and Al data.

Table 4. These and all other olivines analyzed by us in such inclusions are essentially pure forsterite. Again, however, the small size of these crystals makes it difficult to obtain high quality microprobe analyses.

TABLE 4

Electron microprobe analyses of olivine from Murchison inclusions

	1	2
SiO_2	41.48	43.38
Al_2O_3	0.15	0.85
TiO_2	0.01	n.d.*
MgO	55.08	56.27
CaO	0.15	0.22
FeO	0.12	n.d.
V_2O_3	0.01	n.d.
Total	97.00	100.72
	Cations per 4 oxygens	
Mg	1.983	1.946
Fe	0.002	---
Ca	0.004	0.005
Si	1.002	1.007
Al	0.004	0.023
Ti	0.000	---
Total Cations	2.995	2.981

Analysis 1 by wavelength dispersion; 2 by energy dispersion.
(1) OC-1; (2) OC-9.
*n.d. - not detected. Detection limits for minor elements analyzed by wavelength dispersion are (3σ): Fe - 320 ppm, Ti - 310 ppm, V - 140 ppm, Ca - 60 ppm.

Clinopyroxene

Analyses of clinopyroxene are given in Table 5. Pyroxene in the rims of melilite-rich inclusions (columns 1, 2) ranges from titanium-poor aluminous diopside to titaniferous fassaite. They are much more aluminum-rich than the diopside reported by MACDOUGALL (1979) on the rims of spinel-hibonite (SH) inclusions, similar in composition to many pyroxenes in Allende Type B inclusions but less Al- and Ti-rich than the pyroxene reported by MACDOUGALL (1979) from the interior of an SH inclusion.

Pyroxene from spinel-pyroxene aggregates ranges from nearly titanium-free diopside to fassaite. That in OC-9 (columns 5, 6) is very rich in both aluminum and titanium where the pyroxene layer contacts the spinel layer (column 6) but is Al-, Ti-poor away from the spinel (column 5). OC-5 pyroxene shows similar Ti-, Al-enrichment near spinels, but fassaitic grains are too tiny to yield good microprobe analyses. Most pyroxene in OC-5 is similar to that in column 4. Pyroxene in the olivine-pyroxene aggregate OC-1 (column 3) is uniformly low in aluminum and titanium and exhibits no spatial variation in composition from place to place within the inclusion.

Primary pyroxene in the interior of the unusual hibonite-bearing inclusion SH-4 is highly titanium-, aluminum-rich (column 7). Pyroxene grains in the rim of MUCH-1 are again too small for good microprobe analyses but examination of their X-ray spectra shows them to be aluminum-poor diopside. The composition of the aluminous diopside rim on the pink spinel crystal, SP-6, is shown in the final column of Table 5.

Other phases

The feldspathoid-like material that is a major constituent of SH-4 is unusual in two respects. First, feldspathoids and alkali-bearing phases in general are very rare in refractory inclusions in Murchison (MACDOUGALL, 1979). Second, this substance is like no feldspathoid reported from Allende. The analysis in Table 6 (column 1) shows unusually high sodium contents relative to Allende nepheline (*e.g.*, ALLEN *et al.*, 1978) but only minor chlorine or sulfur that would be characteristic of a sodalite-group phase. Variation in the composition and analytical sum of this material suggests that it may not be a single phase. Consistently low totals in the microprobe analyses (75–85%) suggest abundant low-Z elements. Ion microprobe detection of hydrogen by HUTCHEON *et al.* (1980) indicates the presence of water.

The anorthite in the rims of the melilite-rich inclusions is, to our knowledge, the first reported occurrence of this mineral in Murchison refractory inclusions. The thinness of this rim made it difficult to obtain a contamination-free electron microprobe analysis; however, a reasonable analysis is given in Table 6. It is nearly pure anorthite, with no detectable potassium and only a trace of sodium.

TABLE 5

Electron microprobe analyses of clinopyroxene from refractory inclusions in Murchison

	1	2	3	4	5	6	7	8
SiO_2	49.51	34.69	51.68	53.69	52.44	38.87	31.49	42.41
Al_2O_3	9.51	21.63	4.11	2.36	4.64	20.43	22.85	15.91
TiO_2*	0.47	7.42	n.d.†	n.d.	n.d.	5.22	14.22	3.53
MgO	15.41	9.71	19.27	18.01	18.13	10.71	6.04	12.34
CaO	24.95	26.10	22.83	24.93	24.02	24.14	24.22	24.34
Na_2O	n.d.	n.d.	0.47	n.d.	0.50	n.d.	n.d.	n.d.
Total	99.85	99.55	98.36	98.99	99.73	99.37	98.82	98.53
	Cations per 6 oxygens							
Z								
Si	1.787	1.291	1.888	1.951	1.892	1.426	1.183	1.564
Al	0.213	0.709	0.112	0.049	0.108	0.574	0.817	0.436
M1								
Al	0.192	0.240	0.065	0.052	0.089	0.310	0.195	0.255
Mg	0.795	0.539	0.935	0.948	0.911	0.546	0.338	0.647
Ti	0.013	0.208	---	---	---	0.144	0.402	0.098
M2								
Ca	0.965	1.041	0.894	0.971	0.928	0.949	0.975	0.962
Na	---	---	0.033	---	0.035	---	---	---
Mg	0.034	0.000	0.114	0.027	0.064	0.040	0.000	0.032
Total Cations	3.999	4.028	4.041	3.998	4.027	3.989	3.910	3.994

All analyses by energy dispersion. Fe was looked for but not detected in all analyses.
(1) MUM-1; (2) MUM-2; (3) OC-1; (4) OC-5; (5,6) OC-9; (7) SH-4; (8) SP-6.
*Total Ti reported as Ti^{4+}.
†n.d. - not detected.

ORIGINS

Blue spherules

As mentioned above, some of these objects are identical in mineralogy and texture to the cores of the refractory spherules discussed by MACDOUGALL (1981). The recovery procedure used here, however, apparently removes the narrow outer rims of Fe-rich phyllosilicate and diopside which Macdougall observed in the objects which he studied. In addition, our group of blue spherules also includes members which differ in mineralogical composition from those of Macdougall by containing small amounts of melilite and in texture by having hibonite concentrated toward their centers.

TABLE 6

Electron microprobe analyses of an unusual feldspathoid and anorthite from refractory inclusions in Murchison

	1	2
SiO_2	27.87	37.07
Al_2O_3	23.63	38.10
TiO_2	n.d.*	1.03†
MgO	2.30	4.82†
FeO	n.d.	n.d.
CaO	3.38	17.96
Na_2O	24.72	0.22
K_2O	1.51	n.d.
SO_3	0.88	n.a.*
Cl	0.25	n.a.
Total	84.55	99.20

Analyses by energy dispersion.
(1) feldspathoid-like phase in SH-4.
(2) anorthite from rim of MUM-2.
*n.d. - not detected.
†due to contamination from neighboring clinopyroxene.
*n.a. - not analyzed.

Liquid origin. Also as pointed out above, those which do not have hibonite cores have textures which suggest that the hibonite crystals grew in such close proximity to one another that they interfered with one another's growth. Using the same argument that was developed for a Type B1 inclusion in Allende by MACPHERSON and GROSSMAN (1981a) and acknowledging that growth interference textures are not as well developed in the blue spherules as in that inclusion, we suggest that it is very unlikely that the blue spherules formed by condensation of individual crystals in space followed by random accumulation of them into aggregates. Furthermore, the fact that hibonite sometimes forms crystal sprays in which the individual crystals meet on the outermost edges of these inclusions and diverge toward the center, particularly in the inclusion shown by MACDOUGALL (1981), suggests that the hibonite crystals nucleated on the outsides of the inclusions and grew inward. It is difficult to imagine how this could result from condensation of solid hibonite crystals from a vapor, as no pre-existing spheroidal surface existed for the crystals to nucleate upon. It is therefore very unlikely that such inclusions formed by this mechanism. On the other hand, it is easy to understand how these textural features could have resulted from crystallization of a molten droplet in space, as such a droplet would have cooled by radiating heat away from its surface, causing early crystals to nucleate around its exterior (MACDOUGALL, 1981).

Different kinds of cavities in these spherules probably have different origins. In BB-1, for example, many cavities occur within or border on melilite, sug-

gesting that these cavities may have formed by selective reaction of melilite. Other cavities that are associated with fractures or that truncate crystals in an irregular fashion may be polishing artifacts. Finally, cavities not associated with melilite have regular angular shapes, controlled by the flat surfaces of bounding crystals. This type of cavity may have formed by the shrinkage that accompanied crystallization of the blue spherules from melt droplets. Although data for volume change during crystallization of hibonite, spinel, perovskite and gehlenite are not available, it is reasonable to assume that the volume change during crystallization of spherules composed of these phases lies in the range between that of Al_2O_3, 22% (KIRSHENBAUM and CAHILL, 1960), and those of common Ca- or Al-bearing silicates such as anorthite and diopside, 3% and 15%, respectively (YODER, 1976). This is the same order of magnitude as the *total* void space in these inclusions, ~8–10%.

The bulk chemical compositions of BB-1 and BB-2 were determined by combining electron microprobe analyses of their constituent phases with point count modes that were converted to proper volume fractions. BB-1 contains 66% Al_2O_3, 17% MgO, 9% CaO, 6% TiO_2 and 2% SiO_2. BB-2 contains 75% Al_2O_3, 18% MgO, 4% CaO, 3% TiO_2 and 0.1% SiO_2. In order to estimate the temperatures required for melting these inclusions, these analyses were renormalized to 100% CaO + MgO + Al_2O_3 and plotted on the phase diagram for this system determined by RANKIN and MERWIN (1916) which was modified with newer data from GENTILE and FOSTER (1963), NURSE *et al.* (1965) and RAO (1968).

BB-2 plots just to the Ca-rich side of the $MgAl_2O_4$-$CaAl_{12}O_{19}$ join. A liquid of that composition would be expected to begin crystallizing spinel at about 2075°C and spinel + hibonite at about 1780°C. In the pure ternary system, the last liquid would probably disappear at about 1680°C with the appearance of $CaAl_4O_7$. If an inclusion of this composition cooled by radiating heat away from its surface, we might thus expect to find an outer rim of spinel, an inner zone of spinel + hibonite and a small, $CaAl_4O_7$-bearing core. In fact, hibonite and spinel are uniformly distributed in BB-2 which simply means that spinel had not completely encased the droplet before hibonite began crystallizing. The core of BB-2 contains perovskite rather than $CaAl_4O_7$, contrary to the above predictions. Although we know of no experimental data concerning the effect of TiO_2 on the stability of hibonite + perovskite relative to $CaAl_4O_7$, we suspect that its addition to the system CaO-MgO-Al_2O_3 in the amount present in BB-2, 3%, causes the phase field of $CaAl_4O_7$ to shrink due to extensive coupled substitution of Ti^{4+} and Mg^{2+} into hibonite. Table 2 shows that hibonite in BB-2 itself contains over 7% TiO_2 and 4% MgO. STOLPER (pers. comm.) found that Mg-, Ti-bearing hibonite is partially molten at 1600°C, 230° lower than the incongruent melting temperature of pure $CaAl_{12}O_{19}$. Liberally estimating that the presence of TiO_2 will depress all liquidus temperatures by the same amount as the melting point of pure hibonite, we reason that hibonite would begin crystallizing from a melt having the composition of BB-2 at a temperature greater than 1550°C, compared to the above estimate of 1780°C from phase relations in the TiO_2-free system. We have no way of knowing whether BB-2 was ever completely molten, but the euhedral hibonite crystals which show no evidence of resorption indicate that all of the hibonite in this inclusion crystallized from the melt. We have seen that this requires a temperature in excess of 1550°C, probably higher than the temperatures required for complete melting of any of the different types of Allende coarse-grained inclusions studied by BECKETT and GROSSMAN (1982). BB-2 thus contains evidence for the highest temperature so far deduced that was experienced by any refractory inclusion.

BAR-MATTHEWS *et al.* (1982) ruled out a molten origin for BB-5, another refractory inclusion from Murchison, on the basis of the high minimum melting temperature required for it, ~1847°C. Using a more recent phase diagram by NURSE *et al.* (1965), that temperature should be revised downward to 1830°C. We now know that at least one inclusion reached a temperature above 1550°C, making the possibility that BB-5 was once molten slightly more tenable and once again raising the question of the mechanism for producing such high temperatures in the solar nebula. This subject was discussed at length by BAR-MATTHEWS *et al.* (1982) and their arguments will not be repeated. Suffice it to say that hypervelocity collisions between grains of high-temperature condensates in the nebula (KIEFFER, 1975) are more likely to have produced the required temperatures if the nebular gas and the grains within it were still hot at the time of collision (MACDOUGALL, 1981).

A liquid having the same composition as the projection of BB-1's composition into the CaO-Al_2O_3-MgO ternary should begin crystallizing spinel at about 2075°C and produce $CaAl_4O_7$ and $CaAl_2O_4$ before disappearing at 1550°C. Although BB-1 does contain spinel, the other phases present are hibonite, melilite and perovskite, rather than $CaAl_4O_7$ and $CaAl_2O_4$. This is presumably because BB-1 contains a few percent of each of TiO_2 and SiO_2 which, when added to the system CaO-Al_2O_3-MgO, undoubtedly change the phase relations and temperatures from those of the pure ternary. The spinel-rich mantle surrounding the hibonite-rich core of BB-1 indicates that spinel crystallized before hibonite. The irregular shapes of the melilite grains suggest that melilite crystallized from late liquids in the interstices between spinels and hibonites.

Alteration and rimming. MACDOUGALL (1981) reported that each refractory spherule which he studied is rimmed by a layer of hydrous, iron-aluminum-silicate, followed, in most cases, by a narrow layer of

pure diopside. Because the boundary between the iron-rich rim layer and the interior is scalloped and the iron-rich rim phase is certainly not in equilibrium with the iron-free phases, this layer is probably a reaction product between the inclusion and some fluid phase derived from a source rich in oxidized iron. This reaction may have occurred in the Murchison parent body in a low-temperature aqueous alteration process such as that shown to be plausible for Nogoya by BUNCH and CHANG (1980). Any fluids percolating through the parent body would be expected to be very rich in oxidized iron, as the matrix of Murchison contains more than 30 percent FeO (FUCHS *et al.*, 1973). Because the diopside layer on the blue spherules is iron-poor, however, it could not have formed in such a process but must have existed prior to the phyllosilicate rim. In fact, it is characteristic of refractory inclusions in Murchison that magnesian rim phases are very poor in oxidized iron, militating against their formation by interaction with material like the iron-rich matrix phyllosilicates.

An argument against phyllosilicate rim formation by parent body alteration arises, in part, from MACDOUGALL's (1981) observations that rim layers on irregular inclusions are broken, placing spinel and hibonite in direct contact with matrix material. In contrast to the inclusion studied by ARMSTRONG *et al.* (1982), MACDOUGALL (1981) did not find pieces of rim scattered about in the matrix near broken surfaces of the inclusions, implying that breakage did not occur *in situ* and therefore that alteration of refractory inclusions to form phyllosilicates did not occur in the region of the parent body sampled by Murchison. Further, the fragility of the phyllosilicate rims demonstrated in our disaggregation experiments makes it difficult to imagine processes energetic enough to transport the blue spherules from one part of the parent body to another, yet gentle enough to preserve their rims. We thus consider unlikely all models involving alteration of the blue spherules in one parent body site and later transport to the region sampled by Murchison.

We thus turn to the alternative that the blue spherules were rimmed in a solar nebular setting and were incorporated into the parent body during a gentle accretion process, but here also the phyllosilicate must have formed under drastically different conditions than the diopside, *i.e.* at a much lower temperature where both oxidized iron and water can condense. One possibility is that the diopside rim and possibly other rim layers that were later replaced by the iron-rich phyllosilicate (MACDOUGALL, 1981) formed in an analogous way to the well-developed rims on coarse-grained Allende inclusions. In the latter rims, the innermost zone contains iron-rich spinel and perovskite, mantled successively by rims of nepheline + grossular + anorthite, fassaite, diopside and, finally, hedenbergite + andradite. MACPHERSON *et al.* (1981) proposed that this sequence results from metasomatic reaction of the nebular gas with melilite in the interiors of the inclusions. The calcium so released migrated outwards to the gas-solid interface where it reacted with incoming sodium, iron and silicon to form the reaction rims in a diffusion-controlled process involving local equilibrium along chemical potential gradients. One problem in applying this model to the blue spherules, however, is the absence of melilite from the interiors of some of them. Either melilite was completely removed and the cavities are the only record of its previous existence or melilite was never present. In the latter case, if the model of MACPHERSON *et al.* (1981) is applicable, another primary phase must have supplied the calcium. The only ones present are hibonite and perovskite, but there is little textural evidence that these minerals were attacked in alteration reactions. The alternative possibility is that the metasomatism model is not applicable to the blue spherules. In this case, the diopside and possibly other phases that are now replaced by the phyllosilicate simply condensed from the vapor onto the outside of the blue spherules. Because feldspathoids are ubiquitous in the rims on the Allende inclusions, the absence of these sodium-rich phases from the rims on blue spherules is noteworthy. This is further evidence that the latter formed under different physico-chemical conditions from the Allende inclusions.

Chemical composition. Compared to bulk chemical compositions of high-temperature mineral assemblages predicted by equilibrium thermodynamic models to condense from a solar nebular gas, the blue spherules are low in CaO and SiO_2 and high in MgO for their Al_2O_3 contents. If the blue spherules formed by melting of pre-existing aggregates of such high-temperature condensates, the precursor assemblage, like the final crystallization product, was composed predominantly of hibonite, spinel and perovskite. MACDOUGALL (1981) pointed out that the irregular spinel-hibonite inclusions in Murchison (MACDOUGALL, 1979) have both the mineralogical and chemical composition required of the precursor, but textures that indicate that they themselves were not melted. BAR-MATTHEWS *et al.* (1982) pointed out that the abundance of spinel in and absence of melilite from such assemblages is unexpected, as condensation calculations by LATTIMER and GROSSMAN (1978) predict that melilite condenses before spinel in a cooling gas of solar composition. Unpublished calculations by J. M. Lattimer employing newly-determined thermodynamic data for hibonite do not alter this prediction. Thus, it follows from condensation models that inclusions composed of hibonite and melilite with no spinel could have formed by isolation of condensates from the gas above a certain temperature but that spinel-hibonite assemblages with no melilite, like the blue spherules, cannot be readily explained by such models. Even if it is assumed that melilite once filled all of the cavities in the blue spherules before they were altered, the recalculated bulk chemical compositions are only

slightly closer to those of equilibrium condensate assemblages with the proper melilite/spinel ratio. The explanation for the aberrant compositions of the precursors of the blue spherules may be simply that hibonite reacted with the gas to form melilite more slowly than to form spinel, such that, compared to the equilibrium situation, relatively little melilite formed prior to spinel.

Another possible way of attaining the bulk chemical composition of the blue spherules begins with a precursor that has the composition of a compact Type A inclusion, much closer to the composition of an equilibrium condensate assemblage. If this precursor were heated to ~1500°C, it would consist of spinel and a liquid rich in the melilite component (BECKETT and GROSSMAN, 1982). Such material would be unstable against evaporation at that temperature in a gas of solar composition under reasonable nebular pressures. NOTSU *et al.* (1978) showed that MgO, SiO_2 and CaO are preferentially volatilized from melts in the system CaO-MgO-Al_2O_3-TiO_2-SiO_2, leaving high-Al_2O_3 liquids with CaO/Al_2O_3 weight ratios <0.5. If the volatilization rate of the liquid were much greater than that of its coexisting spinel, the result could be a spinel + liquid mixture with the same bulk composition as a blue spherule. The success of this process in achieving the desired composition depends upon preventing spinel from dissolving in the melt and upon the degree to which the MgO locked up in the spinel is thereby protected from evaporation. Recall that spinel coexists with liquid below 2075°C in systems with the bulk composition of the blue spherules. It is thus quite conceivable that, given the right combination of heating and evaporation rates, there would always be solid spinel in the liquid as the latter changed composition. COHEN (1981) was the first to mention the possibility that CaO might separate from Al_2O_3 during partial melting of refractory assemblages and volatilization of the liquid so produced.

In summary, a model for formation of blue spherules which is consistent with all of our observations is condensation of high-temperature minerals, accretion of these phases into nodules, melting of these nodules into droplets in high energy processes in the solar nebula, crystallization of the droplets and, finally, lower-temperature interaction of the inclusions with the nebular gas, producing an outer rim sequence. The blue spherules could have achieved their bulk compositions if the condensation process deviated from equilibrium or, in case the condensation step did occur at equilibrium, if the inclusions were only partially melted afterwards and significant volatilization from the melt accompanied that event.

Melilite-rich inclusions

Primary phases. Of all the types of refractory inclusions we have studied in Murchison, this group is the most similar to any described from Allende. Although the greater abundance of hibonite and higher gehlenite content of the melilite combine to make the melilite-rich inclusions more aluminous, the texture and mineralogy of the primary phase assemblage of these inclusions are identical to those of Allende compact Type A inclusions. Unfortunately, however, the latter have so far yielded few petrographic or mineralogical clues to their origin. Although they are composed of high-temperature condensate minerals, there is no definitive evidence as to whether they formed by direct condensation of solids from the solar nebular gas or whether they were molten during or after condensation. In the Murchison melilite-rich inclusions themselves, hibonite and perovskite, phases predicted to condense prior to melilite in a cooling gas of solar composition, tend to be concentrated toward the outsides. Furthermore, their compact structure indicates that they could not have formed by random aggregation of completely-grown crystals that had condensed independently in space. Considered together, these arguments might be taken to mean that these objects are not direct solid condensates from a gas but, instead, may have crystallized from melt droplets. On the other hand, it is certainly conceivable that condensation of individual crystals, chains, sheets and clumps of hibonite, perovskite and spinel was followed by condensation of melilite before, during and after accretion such that overgrowth of melilite filled the interstices of the aggregates to produce a compact mass. In this case, the gross spatial distribution of the phases need not bear a close relationship to the sequence in which they condensed. A difficulty for the condensation model, however, is that spinels are poikilitically enclosed within individual melilite crystals, implying that spinel condensed before melilite. The problem is that thermodynamic calculations predict the opposite sequence, the same difficulty encountered in the origin of blue spherules. One solution offered in that discussion may also be applicable here, that the reaction of hibonite with the gas to form melilite may be kinetically hindered, causing hibonite to react to form spinel first.

Alteration and rimming. In the melilite-rich Murchison inclusions, cavities are present in the melilite, some of which contain no secondary phases and others of which are filled with calcite and iron sulfide. Absent from these inclusions are the veins of feldspathoid- and grossular-rich alteration products so typical of all coarse-grained inclusion types in Allende. In contrast to the well-developed rims found on many Allende inclusions, the rims on Murchison melilite-rich inclusions lack a layer rich in feldspathoids and grossular, lack one rich in andradite and hedenbergite and contain a layer of massive melilite and another of massive anorthite. Although the presence of sodium and oxidized iron in the rims on Allende inclusions is not taken to imply that those rims formed by reaction of the inclusions with the Allende matrix, the absence of these components

from the observed rims of the melilite-rich inclusions negates the possibility that the latter rims formed by reaction of the inclusions with the Murchison matrix, whether or not any undetected rim layers were lost during recovery. We suggest that the rim sequence on the Murchison melilite-rich inclusions formed by a process broadly similar to that proposed by MACPHERSON *et al.* (1981) for Allende inclusions. The above-mentioned differences between the rim sequences on inclusions from the two meteorites imply that physico-chemical conditions of melilite alteration and rim deposition were different for each population. Indeed, mineralogical differences between the rims on melilite-rich inclusions and those on blue spherules, both from Murchison, also reflect differences in physico-chemical conditions of rim deposition. Straightforward interpretation of the presence of melilite as a rim layer on the melilite-rich inclusions in terms of the MACPHERSON *et al.* (1981) model would seem to require that melilite was both a reactant and a product of the same chemical reaction. This is impossible, but a plausible alternative is that a melilite-free rim sequence began to develop in the way envisioned by the model, but was modified when a small change in the temperature, pressure or composition of the gas phase restabilized melilite relative to other rim phases, causing a melilite layer to form at their expense. Another possibility is that the melilite rim was deposited during a condensation event and that the other rim layers on the Murchison melilite-rich inclusions formed by alteration of it.

We suspected that some cavities in the melilite are artifacts of our freeze-thaw disaggregation process, since the ultrasonic agitation step tends to warm the water used therein. Hot water extracts of Murchison were found by FUCHS *et al.* (1973) to contain Ca and Al, and we thought that other soluble components in Murchison might make the water acidic, enhancing the solubility of melilite. Experiments were conducted on fresh melilite to test this possibility and no sign of etching was detected.

Other hibonite-bearing inclusions

MUCH-1. The structure of MUCH-1 is dominated by a radial aggregate of hibonite crystals mantled by rim layers that, by virtue of the scalloped appearance of the hibonite surfaces, must be replacing the latter phase. Because hibonite appears so early in the condensation sequence, inclusions formed by direct condensation of solids might be expected to contain hibonite-rich cores and mantles of lower temperature condensates. Heterogeneous nucleation in a low density gas could easily lead to spherulitic aggregates in the case of a phase such as hibonite that forms elongate or platy crystals.

It is difficult to imagine how crystallization of a liquid droplet could result in an object having the highly irregular shape seen in Fig. 4, as opposed to something more nearly spheroidal. If, however, it is assumed that MUCH-1 formed by crystallization of a near-spherical droplet having a radius equal to the length of the largest hibonite crystal, the portion of that sphere now occupied by hibonite crystals and the bands of alteration products concentric with them is only 25 percent by volume. This requires that the volume change on crystallization of the putative droplet must have been 75 percent, far in excess of any reasonable value. This argument assumes that the black phyllosilicate material surrounding the radial structure is not itself an alteration product of primary phases which solidified from the same liquid as the hibonite. This is a reasonable assumption, as the only candidates for such phases in the system CaO-Al_2O_3-MgO-SiO_2 can each be ruled out: spinel because of its resistance to alteration; $CaAl_4O_7$ because of its chemical and thermodynamic similarity to hibonite which is resistant to alteration; melilite and anorthite because they are not altered to phyllosilicates in other Murchison inclusions; clinopyroxene because its presence as a rim layer means that it is a product, rather than a victim, of alteration of this inclusion; and glass because the difficulty of quenching such a low-SiO_2 liquid makes it unlikely that this phase was ever present. We thus conclude that the hibonite aggregate of MUCH-1 did not crystallize from a melt but formed instead by direct condensation from a vapor. ARMSTRONG *et al.* (1982) concluded that the Blue Angel inclusion, a porous object similar in some respects to MUCH-1, is a nebular condensate except for its secondary alteration products, but those workers were unable to determine whether their inclusion condensed as a liquid droplet or as an assemblage of solid phases.

The fact that the hibonite crystals in MUCH-1 have scalloped margins and are mantled faithfully by successive layers of calcite + gypsum, perovskite, Fe-rich phyllosilicate and, finally, diopside indicates that hibonite has reacted with a fluid phase or phases to form these minerals. As in the case of the blue spherules, the diopside rim could not have formed in the same process as the phyllosilicate. Perhaps it is a vestige of a more extensive rim sequence that formed at relatively high temperature in the solar nebula *via* the mechanism proposed by MACPHERSON *et al.* (1981). Later and at much lower temperature, this rim sequence and possibly more of the hibonite could have been partially altered to form the other rim layers observed. In this respect, our model for the history of MUCH-1 is similar to that proposed by ARMSTRONG *et al.* (1982) for the Blue Angel inclusion. There is no direct textural evidence in MUCH-1 that bears on the question of whether this low-temperature alteration occurred prior to or after incorporation of MUCH-1 into the meteorite parent body. ARMSTRONG *et al.* (1982) proposed that the Blue Angel underwent alteration in one region of the parent body and was later transported to the place where it was found by volcanic or impact processes. The fact that the delicate structure of MUCH-1 is at least

partially preserved, however, argues against its transport from one place in the parent body to another in such energetic events. The low-temperature stage of the alteration of MUCH-1 occurred either *in situ* or in the solar nebula.

There is no question that some gypsum was deposited after formation of the Murchison parent body, as veins of this phase are known to occur in this meteorite (FUCHS *et al.*, 1973). Coupled with the fact that both gypsum and calcite are water soluble, this suggests that these phases may have precipitated from aqueous solutions that once percolated through the parent body. The origin of the solutes in such solutions is not known. All matter in C2 chondrites ultimately owes its origin to condensation processes in the solar nebula which, at low temperature, may very well be capable of producing such phases as calcite and gypsum. Because of this possibility, the aqueous solutions may have acquired their solutes within the parent body by dissolving such nebular calcite and gypsum, some of which may have escaped dissolution and are still preserved. Thus, in the case of a particular inclusion such as MUCH-1 in which there is no direct evidence for the timing of low-temperature alteration relative to accretion, condensation is a viable alternative to deposition from aqueous solutions in the parent body as a hypothesis for the formation of gypsum and calcite.

ARMSTRONG *et al.* (1982) pointed out that if åkermanite were exposed to a gas containing CO_2 at partial pressures that might be expected for this species in the solar nebula, calcite and diopside would be stable reaction products only below 98°K, a temperature so low that the reaction would be prevented by kinetics. On the basis of this argument alone, they rejected the possibility that $CaCO_3$ could have formed by condensation processes in the solar nebula. This conclusion is premature. The proper way of investigating calcite stability in the solar nebula is by means of complete, systematic condensation calculations, in which the equilibrium distribution of the elements between all gaseous species and crystalline phases is calculated at each temperature in such a way that the possibility of calcite formation by all possible reaction paths is automatically assessed. Despite the success of such calculations at high temperatures, they have not been performed in the necessary detail below 1000°K because of their vastly greater complexity at low temperatures. Extrapolations of high-temperature calculations suggest that calcite stability in the solar nebula would not be expected above 500°K. It may be that all of the rim phases on MUCH-1 except diopside formed by reaction with the solar nebular gas in the temperature range 300–400°K and that the mineralogical differences between the rims on MUCH-1 and those on other inclusions are related to differences in the temperature of rim formation.

It could be argued that unfavorable kinetics might have prevented calcite from forming even at these temperatures, assuming that it has a stability field. The mere existence of calcite in carbonaceous chondrites, however, argues that carbon was able to condense from the solar nebula under some conditions in some oxidized form, perhaps as calcite itself. It could also be argued that any Al-rich, high-temperature inclusion that had been exposed to the gas at a temperature low enough for calcite to have formed as an alteration product should also contain Na-rich alteration products like feldspathoids that would have formed at an intermediate temperature. Some refractory inclusions such as MUCH-1, however, may have condensed in a different part of the solar nebula from the low-temperature components of Murchison and may have mixed with the latter after all of the sodium, but not the CO_2, had already condensed in the region where the low-temperature material had formed. A requirement of this explanation is that the process that brought these components together was rapid enough to prevent back-reaction of hibonite at intermediate temperature.

SH-4. Although the fassaite in SH-4 implies a similarity to Allende Type B inclusions, the great abundance of spinel and presence of hibonite suggest that this inclusion is more aluminous than those objects. In fact, the unusual feature of SH-4 is that it contains large, primary crystals of both fassaite and hibonite as essential phases. Coexistence of these two minerals as primary phases is not known from any other Murchison inclusion and has been reported only once from an Allende inclusion (ALLEN *et al.*, 1978). Because of the intense alteration of SH-4, it is almost impossible to determine whether the primary phases were once snugly intergrown with one another, which might imply a liquid origin, or were loosely held together, which might imply that SH-4 is an aggregate of condensate grains and possibly other particles with different origins. From phase relations in the system CaO-Al_2O_3-MgO-SiO_2, it is conceivable that crystallization of hibonite and spinel from an Al_2O_3-rich, SiO_2-bearing melt could lead to eventual crystallization of pyroxene. This is consistent with the fact that spinels are poikilitically enclosed by pyroxene in SH-4. Although the generally spherical outline of the inclusion argues against formation by aggregation, the intensity of the alteration implies that the object was originally very porous, rather than compact.

The primary phase assemblage of SH-4 is similar to that of the other refractory inclusions discussed so far. All of these inclusions were once in close proximity to one another in the parent body. Had they all been altered by reaction with fluids at that time, all of them should have had the same components added to them during this process. SH-4 is the only inclusion which we have studied, however, that contains a major, sodium-bearing alteration product. The fact that none of the other refractory inclusions contain feldspathoids implies that SH-4 obtained its sodium prior to incorporation into the same region

of the parent body as the other refractory inclusions. Furthermore, if alteration of the Murchison refractory inclusions occurred in the solar nebula, SH-4 was altered in a different place or at a different time. SH-4 is also the only inclusion discussed so far that has a rim layer of forsterite, an FeO-free phase that could not have formed by *in situ* reaction. Thus, if SH-4 were altered in the solar nebula, the forsterite rim is further evidence that this process occurred in a different region or at a different time from the other refractory inclusions. Although we cannot rule out the possibility that all of the inclusions once had forsterite rims which were later replaced by phyllosilicates, there is no clear textural or chemical evidence for any reaction relationship between the forsterite rim of SH-4 and the surrounding phyllosilicate bands.

Spinel-pyroxene and olivine-pyroxene inclusions

These objects are composed predominantly of phases predicted to be high-temperature condensates from the solar nebula: perovskite and Fe-free spinel, olivine and pyroxenes. The structures of the banded objects could not have resulted from crystallization of a melt. Such a model could not work for the nodular ones, either, even if nodules formed by solidification of droplets were later sintered together. Such droplets would have been so rich in the spinel component that spinel would have been the first phase to crystallize, and each nodule in the final sintered aggregate would have a spinel rim and a clinopyroxene-rich core—the opposite of what is observed. It is more likely that these aggregates formed by condensation and heterogeneous nucleation of spinel in the solar nebula, whereby crystals nucleated and grew on the surfaces of earlier formed crystals, thus forming chains, sheets and nodules of spinel.

Unexplained in such a model is the absence of hibonite and melilite, calcium-rich phases with condensation temperatures comparable to the phases present. It is possible, however, that the prominent rims of clinopyroxene are replacement products of melilite that once mantled the spinel nodules and sheets and that perhaps also once filled cavities within the spinel. Even if the cavities were once filled with melilite, the ratio of melilite to spinel would still be lower than expected for an equilibrium condensate assemblage, as in the blue spherules. Unlike the rim sequences described by WARK and LOVERING (1977) on Allende inclusions, however, there is no compelling evidence that the clinopyroxene bands in the spinel-pyroxene inclusions are related to the alteration of melilite. An alternative model is that clinopyroxene simply condensed on the spinel structures. Likewise, the forsterite and enstatite rims may have condensed sequentially on top of the clinopyroxene bands. The absence of sodium and oxidized iron from these rim layers suggests formation temperatures above ~900°K at 10^{-3} atm. total pressure. The small amounts of troilite and phyllosilicates present in these inclusions must have been introduced in a later, lower-temperature event. In models where the clinopyroxene does not replace an earlier calcium-rich phase, the problem remains of why hibonite and melilite are missing.

There are obvious mineralogical and textural similarities between the botryoidal spinel-pyroxene aggregates and the olivine-pyroxene one. We have not yet seen enough of these to tell whether there is a complete gradation between spinel-rich and spinel-free aggregates or whether there are some characteristics common to the spinel-free ones which distinguish them from spinel-rich ones. The most that can be said about the spinel-free one at the present time is that it is composed predominantly of minerals predicted to condense from the solar nebula between 1275° and 1450°K at a total pressure of 10^{-3} atm. and it has a structure that does not appear to be readily explainable by crystallization from a liquid. It may be an aggregate of minerals which condensed directly as solids.

Diopside-rimmed spinel nodules identical to some of the objects seen here have been described in micrometeorites collected from deep sea sediments by BROWNLEE *et al.* (1980). This, together with the fact that these spinel-pyroxene aggregates have never been observed in C1 or C3 chondrites, lends support to the idea that the micrometeorite population contains particles that were derived from the same source as C2 chondrites and further, to the extent that micrometeorites are cometary in origin, that the comets contain the same high-temperature condensate aggregates as C2 chondrites.

Individual hibonite and spinel crystals

These objects were either incorporated as individual crystals during accretion of the Murchison parent body or were released from relatively fragile inclusions during gardening on the parent body or later freeze-thaw disaggregation. The blue spherule interiors and melilite-rich inclusions are so compact that they tend to survive the freeze-thaw process intact. Even if some of these did fragment during this process or during gardening, it is unlikely that individual spinel or hibonite crystals so free of attached material would be released. On the other hand, fragile inclusions like MUCH-1 would not be expected to survive either gardening or the disaggregation process intact. The similarly low TiO_2 and MgO contents of the individual hibonite crystals and those in MUCH-1 lends support to the hypothesis that inclusions like MUCH-1 were the original hosts of the individual ones. If this is true, it is puzzling that no hibonite chips with high TiO_2 and MgO contents were recovered, as MACDOUGALL (1979) reported such hibonite from inclusions that appear to be at least as fragile as MUCH-1. Furthermore, the individual hibonite that is rimmed by chromium-rich spinel also has the

same composition as the other individual hibonite crystals; yet, spinel of that composition is not present in MUCH-1, suggesting that there is at least one other possible source for the individual hibonites. In fact, chrome-rich spinel has not been found with other phases in any refractory inclusion either by us or MACDOUGALL (1979, 1981).

Although the single blue spinel octahedron has the same composition as spinel in most refractory inclusions which we have studied in Murchison, it is so much larger than the spinel crystals seen inside any of those inclusions that they are unlikely sources for it. The lack of adhering material further supports the idea that it was never part of a larger inclusion. Perhaps it condensed from the solar nebula but was never incorporated into a larger inclusion prior to accretion of the parent body. In contrast, the pink and red spinels often occur in association with aluminous diopside and sometimes forsterite, suggesting that the ones we have studied are fragments of the olivine- and pyroxene-rich inclusions studied by FUCHS *et al.* (1973) which are known to contain accessory chrome-bearing spinel.

CONCLUSIONS

We have described a number of types of refractory inclusions from the Murchison C2 chondrite that are related, but not identical, to those in Allende. The melilite-rich inclusions are similar to coarse-grained compact Type A inclusions in Allende, but are more aluminous. Similarly, SH-4 is reminiscent of Allende Type B inclusions in containing primary fassaite, but is more aluminous than these. The blue spherules tell us unambiguously that some refractory inclusions were subjected to higher temperatures than have been deduced from any Allende inclusion. Also, the structures of MUCH-1 and the spinel-pyroxene aggregates are probably the result of direct condensation of solids from the vapor of the solar nebula, a process for which clear textural evidence is elusive in refractory inclusions from Allende.

The processes that affected the Murchison inclusions after their primary solidification have left their mark in a bewildering array of alteration products and rim sequences. Iron-free phases such as diopside, fassaite, forsterite and enstatite are important rim constituents on all types of inclusions studied here. These phases could not have formed by reaction of the inclusions with the iron-rich matrix material of the parent body or fluids derived therefrom but must have formed in the solar nebula. The origins of such phases as feldspathoids, calcite, gypsum and phyllosilicates found either as alteration products in inclusion interiors or rim layers on their surfaces is less clear. Direct evidence for *in situ* formation of the latter phases, such as veins which cross-cut the inclusions, is totally absent. In fact, for some inclusions, there is good evidence that these phases formed prior to emplacement of the inclusions into the positions in which they were found. If they were altered during processes inside of a parent body, it is necessary that they were widely separated in space at that time and that they were then all brought into close proximity to one another to form the rock which we call the Murchison meteorite. If MUCH-1 were one of the inclusions which were transported, its fragility imposes severe constraints on the nature of the emplacement process. Instead, it may be that the feldspathoids, calcite, gypsum and phyllosilicates also formed by reaction of the inclusions with the solar nebular gas. Our work suggests that some inclusions were exposed to the gas under different physicochemical conditions from others, presumably at different times and in different places. It also suggests that individual inclusions may have experienced alteration processes in more than one nebular environment.

Acknowledgments—We thank R. N. Clayton, A. M. Davis, I. Hutcheon, I. Kawabe, R. C. Newton, E. Stolper and B. J. Wood for helpful discussions. V. Ekambaram helped with the etching experiments. J. M. Lattimer and E. Stolper kindly provided unpublished data. This work was supported by the National Aeronautics and Space Administration through grants NGR 14-001-249 (to L. Grossman) and NAGW-23 (to E. Olsen). Parts of this paper were written by L. Grossman while on leave at the Hebrew University of Jerusalem where he was supported by funds from the Lady Davis Fellowship Trust and funds from Mr. Lester M. Finkelstein.

REFERENCES

ALLEN J. M., GROSSMAN L., DAVIS A. M. and HUTCHEON I. D. (1978) Mineralogy, textures and mode of formation of a hibonite-bearing Allende inclusion. In *Proc. Lunar Planet. Sci. Conf. 9th*, 1209–1233.

ARMSTRONG J. T., MEEKER G. P., HUNEKE J. C. and WASSERBURG G. J. (1982) The Blue Angel: I. The mineralogy and petrogenesis of a hibonite inclusion from the Murchison meteorite. *Geochim. Cosmochim. Acta* **46**, 575–595.

BAR-MATTHEWS M., HUTCHEON I. D., MACPHERSON G. J. and GROSSMAN L. (1982) A corundum-rich inclusion in the Murchison carbonaceous chondrite. *Geochim. Cosmochim. Acta* **46**, 31–41.

BECKETT J. R. and GROSSMAN L. (1982) Melting experiments on Allende coarse-grained inclusion compositions (abstract). In *Lunar and Planetary Science XIII*, pp. 31–32. The Lunar and Planetary Institute.

BROWNLEE D. E., BATES B. A., PILACHOWSKI L. B., OLSZEWSKI E. and SIEGMUND W. A. (1980) Unmelted cosmic materials in deep sea sediments (abstract). In *Lunar and Planetary Science XI*, pp. 109–111. The Lunar and Planetary Institute.

BUNCH T. E. and CHANG S. (1980) Carbonaceous chondrites—II. Carbonaceous chondrite phyllosilicates and light element geochemistry as indicators of parent body processes and surface conditions. *Geochim. Cosmochim. Acta* **44**, 1543–1577.

COHEN R. E. (1981) Refractory inclusions in the Mokoia C3 (V) carbonaceous chondrites (abstract). *Meteoritics* **16**, 304.

EL GORESY A., RAMDOHR P. and NAGEL K. (1980) A unique inclusion in Allende meteorite: a conglomerate of hundreds of various fragments and inclusions (abstract). *Meteoritics* **15**, 286–287.

FUCHS L. H., OLSEN E. and JENSEN K. (1973) Mineralogy,

mineral-chemistry, and composition of the Murchison (C2) meteorite. *Smithson. Contrib. Earth Sci.* No. 10, 39 pp.

GENTILE A. L. and FOSTER W. R. (1963) Calcium hexaluminate and its stability relations in the system CaO-Al_2O_3-SiO_2. *J. Amer. Ceramic Soc.* **46**, 74–76.

GROSSMAN L. (1972) Condensation in the primitive solar nebula. *Geochim. Cosmochim. Acta* **36**, 597–619.

GROSSMAN L. (1975) Petrography and mineral chemistry of Ca-rich inclusions in the Allende meteorite. *Geochim. Cosmochim. Acta* **39**, 433–454.

GROSSMAN L. (1980) Refractory inclusions in the Allende meteorite. *Ann. Rev. Earth Planet. Sci.* **8**, 559–608.

HUTCHEON I. D., BAR-MATTHEWS M., TANAKA T., MACPHERSON G. J., GROSSMAN L., KAWABE I. and OLSEN E. (1980) A Mg isotope study of hibonite-bearing Murchison inclusions (abstract). *Meteoritics* **15**, 306–307.

KEIL K. and FUCHS L. H. (1971) Hibonite [$Ca_2(Al,Ti)_{24}O_{38}$] from the Leoville and Allende chondritic meteorites. *Earth Planet. Sci. Lett.* **12**, 184–190.

KIEFFER S. W. (1975) Droplet chondrules. *Science* **189**, 333–340.

KIRSHENBAUM A. D. and CAHILL J. A. (1960) The density of liquid aluminum oxide. *J. Inorg. Nuclear Chem.* **14**, 283–287.

LATTIMER J. M. and GROSSMAN L. (1978) Chemical condensation sequences in supernova ejecta. *The Moon and the Planets* **19**, 169–184.

LEE T. (1979) New isotopic clues to solar system formation. *Rev. Geophys. Space Phys.* **17**, 1591–1611.

MACDOUGALL J. D. (1979) Refractory-element-rich inclusions in CM meteorites. *Earth Planet. Sci. Lett.* **42**, 1–6.

MACDOUGALL J. D. (1981) Refractory spherules in the Murchison meteorite: Are they chondrules? *Geophys. Res. Lett.* **8**, 966–969.

MACPHERSON G. J. and GROSSMAN L. (1979) Melted and non-melted coarse-grained Ca-, Al-rich inclusions in Allende (abstract). *Meteoritics* **14**, 479–480.

MACPHERSON G. J. and GROSSMAN L. (1981a) A once-molten, coarse-grained, Ca-rich inclusion in Allende. *Earth Planet. Sci. Lett.* **52**, 16–24.

MACPHERSON G. J. and GROSSMAN L. (1981b) Clastic rims on inclusions: Clues to the accretion of the Allende parent body (abstract). In *Lunar and Planetary Science XII*, pp. 646–647. The Lunar and Planetary Institute.

MACPHERSON G. J., GROSSMAN L., ALLEN J. M. and BECKETT J. R. (1981) Origin of rims on coarse-grained inclusions in the Allende meteorite. *Proc. Lunar Planet. Sci. Conf. 12B*, 1079–1091.

MACPHERSON G. J., BAR-MATTHEWS M., TANAKA T., OLSEN E. and GROSSMAN L. (1980) Refractory inclusions in Murchison: Recovery and mineralogical description. In *Lunar and Planetary Science XI*, pp. 660–662. The Lunar and Planetary Institute.

NOTSU K., ONUMA N., NISHIDA N. and NAGASAWA H. (1978) High temperature heating of the Allende meteorite. *Geochim. Cosmochim. Acta* **42**, 903–907.

NURSE R. W., WELCH J. H. and MAJUMDAR A. J. (1965) $CaO-Al_2O_3$ system in a moisture-free atmosphere. *Trans. Brit. Ceramic Soc.* **64**, 409–418.

RANKIN G. A. and MERWIN H. W. (1916) The ternary system $CaO-Al_2O_3$-MgO. *Amer. Chem. Soc. J.* **38**, 568–588.

RAO M. R. (1968) Liquidus relations in the quaternary subsystem $CaAl_2O_4$-$CaAl_4O_7$-$Ca_2Al_2SiO_7$-$MgAl_2O_4$. *J. Amer. Ceramic Soc.* **51**, 50–54.

WARK D. A. and LOVERING J. F. (1977) Marker events in the early evolution of the solar system: Evidence from rims on Ca-Al-rich inclusions in carbonaceous chondrites. In *Proc. Lunar Sci. Conf. 8th*, 95–112.

YODER H. S. JR. (1976) *Generation of Basaltic Magma*. National Academy of Sciences, 265 pp.